Electronic Supplementary Material (ESI) for Journal of Materials Chemistry C.
This journal is © The Royal Society of Chemistry 2023

Efficient energy transfer from crystalline silicon to Erbium

(Supplementary Information)

Huan Liu[1], Ulrich Kentsch[2], Fangyu Yue[3], Abdelmadjid Mesli[4] and Yaping Dan[1]

[1] University of Michigan-Shanghai Jiao Tong University Joint Institute, Shanghai Jiao Tong University, Shanghai, 200240, China.

[2] Institute of Ion Beam Physics and Materials Research, Helmholtz-Zentrum Dresden – Rossendorf, Dresden 01328, Germany.

[3] Key Laboratory of Polar Materials and Devices, Ministry of Education, East China Normal University, Shanghai, 200241, China.

[4] Institut Matériaux Microélectronique Nanosciences de Provence, UMR 6242 CNRS, Université Aix-Marseille, 13397 Marseille Cedex 20, France.

I Sample preparations

The uniform profile of Er/O/B is obtained by several implantations with parameters listed below: (tilt angle 7 degrees)

Erbium: Er concentration is fixed for all the samples

Concentration (cm^{-3})	**Energy (keV)/ Dose (cm^{-2})**	**Energy (keV)/ Dose (cm^{-2})**	**Energy (keV)/ Dose (cm^{-2})**	**Energy (keV)/ Dose (cm^{-2})**	**Energy (keV)/ Dose (cm^{-2})**
8.7E+20	40/1.1E+15	80/1.2E+15	140/2.0E+15	240/2.5E+15	400/6.1E+15

Oxygen: O concentration is varied from 6.3E+20 to 3.3E+21 with proportionally scaled doses and same energies listed below.

Concentration (cm^{-3})	**Energy (keV)/ Dose (cm^{-2})**	**Energy (keV)/ Dose (cm^{-2})**	**Energy (keV)/ Dose (cm^{-2})**	**Energy (keV)/ Dose (cm^{-2})**	**Energy (keV)/ Dose (cm^{-2})**	**Energy (keV)/ Dose (cm^{-2})**
1.6E+21	10/3.1E+15	20/3.9E+15	30/3.1E+15	40/5.0E+15	60/6.3E+15	65/1.3E+15

Boron: B concentration is varied from 3.84E+19 to 3.3E+21 with proportionally scaled doses and same energies listed below.

Concentration (cm^{-3})	**Energy (keV)/ Dose (cm^{-2})**	**Energy (keV)/ Dose (cm^{-2})**	**Energy (keV)/ Dose (cm^{-2})**

7.7E+19	10/2.2E+14	20/3.7E+14	40/1.0E+15

Secondary-ion Mass Spectrometry (SIMS)

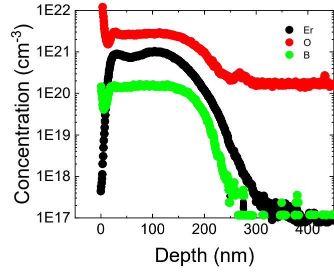

Figure S1: Depth profile of Er/O/B concentrations in sample S_1.

II Fabrication optimization

The normalized PL intensity and PL decay rate for samples Group-O and Group-B, as well as the annealing condition optimization results.

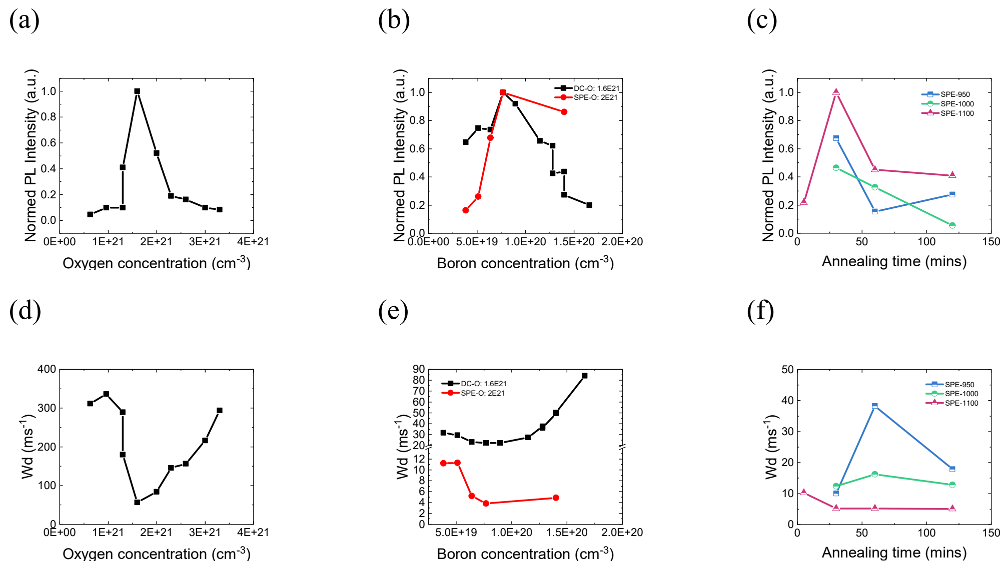

Figure S2: Optimization of dopants concentration and solid phase epitaxy conditions based on PL intensity (a-c) and decay rate W_d (d-f). (a, d) DC-processed samples with different oxygen concentration and none boron doping. (b, e) DC-processed (black, O concentration 1.6×10^{21}cm^{-3}) and SPE-processed (red, O concentration 2.0×10^{21}cm^{-3}) samples with different boron concentrations. (c, f) SPE-processed samples with different annealing temperatures (blue: 950°C, green: 1000°C, red: 1100°C) and times.

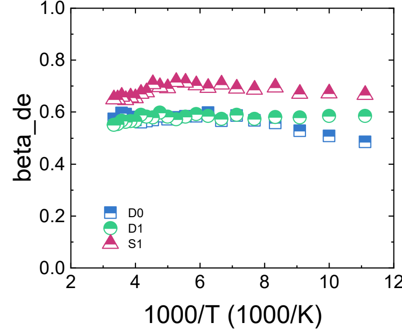

Figure S3: The fitted beta values at different temperatures for samples D_0, D_1, S_1.

III Derivations of ϕ_{out}

From rate equations **eq. (2-3)** in the main text, in the steady-state,

$$\eta_{trap}G = n_{Er}(W_{SRH} + W_{fd}) - N_{Er}W_{bt} \quad (1)$$

$$n_{Er}W_{fd} = N_{Er}W_{d} \quad (2)$$

Then we have

$$N_{Er} = \frac{\eta_{trap}GW_{fd}}{W_0W_{fd} + W_{SRH}W_d} \quad (3)$$

The excited erbium ions N_{Er} can be related to the output photo-flux density through

$$\phi_{out} = CW_{rad}tN_{Er} \quad (4)$$

in which W_{rad} is the constant radiative recombination rate of erbium ions (fixed as 0.5ms^{-1}), t is the thickness of the Er active region, C is the collection efficiency of our PL measurement system. Therefore, the measured photo-flux can be written as

$$\frac{1}{\phi_{out}} = \frac{W_0W_{fd} + W_{SRH}W_d}{CW_{rad}t\eta_{trap}GW_{fd}} = A(W_0W_{fd} + W_{SRH}W_d) \quad (5)$$

In which

$$A = \frac{1}{CW_{rad}t\eta_{trap}GW_{fd}} \quad (6)$$

$$W_d = W_{bt0}\exp\left(-\frac{E_a}{k_BT}\right) + W_0 \quad (7)$$

IV Derivations of W_{SRH}

Shockley-Read-Hall recombination rate for photo-generated excess carriers through a defect state is

$$\frac{dn}{dt} = U = \frac{N_t r_n r_p (np - n_i^2)}{r_n(n + n_1) + r_p(p + p_1)} \# \quad (8)$$

The electron concentration at this defect state should be

$$n_t = \frac{N_t(nr_n + p_1 r_p)}{r_n(n + n_1) + r_p(p + p_1)} \# \quad (9)$$

, in which N_t is the defect density; r_n, r_p are the electron, hole capture coefficients, which barely changes in the temperature range (80-300K) we discuss; $n = n_0 + \Delta n$, $p = p_0 + \Delta p$ are the total electron and hole concentrations; n_0, p_0 are the corresponding carrier concentrations at equilibrium; $\Delta n = \Delta p$ is the excess carrier concentration generated by optical excitation; n_1, p_1 are defined as follows,

$$n_1 = N_c \exp\left(-\frac{E_c - E_t}{k_B T}\right) \# \quad (10)$$

$$p_1 = N_v \exp\left(-\frac{E_t - E_v}{k_B T}\right) \# \quad (11)$$

, in which N_c, N_v are the effective density of states of CBM E_c and VBM E_v, E_t is the defect energy level. For n-type (verified by Hall measurements in Figure S4) material (which means $n > n_0 \gg p, p_1 > p_0$, $E_t > E_i$), under the low-injection condition ($n_0 \gg \Delta n = \Delta p \gg p_0$), we have

$$np - n_i^2 = (n_0 + \Delta n)(p_0 + \Delta p) - n_i^2 = (n_0 + p_0)\Delta n + \Delta n^2 \approx n_0 \Delta n \# \quad (12)$$

Then eq. (8), (9) can be simplified as

$$\frac{dn}{dt} = \frac{N_t r_p n_0 \Delta n}{n_0 + n_1} \# \quad (13)$$

$$n_t = \frac{N_t n}{(n + n_1)} \# \quad (14)$$

SRH recombination rate W_{SRH} for n_t should be

$$\frac{dn_t}{dt} = \frac{N_t n_1}{(n + n_1)^2} \frac{dn}{dt} \approx \frac{N_t n_1}{(n_0 + n_1)^2} \frac{dn}{dt} \# \quad (15)$$

Applying eq. (13) we can get

$$\frac{dn_t}{dt} = \frac{N_t^2 r_p n_0 \Delta n n_1}{(n_0 + n_1)^3} = \frac{N_t^2 r_p \Delta n}{n_0} \frac{n_1/n_0}{(1 + n_1/n_0)^3} \# \quad (16)$$

For highly-degenerate material, high n_0 is obtained, which barely changes when the temperature is varied (verified by Hall measurements in Figure S4), so we have $\frac{n_1}{n_0} \ll 1$, thus

$$W_{SRH} = \frac{dn_t}{dt} \approx \frac{N_t^2 r_p \Delta n}{n_0^2} n_1 = \frac{N_t^2 r_p \Delta n N_c}{n_0^2} \exp\left(-\frac{E_c - E_t}{k_B T}\right) = \frac{A N_c}{n_0^2} \exp\left(-\frac{E_c - E_t}{k_B T}\right) \quad (17)$$

, in which $A = N_t^2 r_p \Delta n$ is a constant at a fixed pumping photoflux density.

V Hall measurements

Our Er/O/B co-doped sample is n-type material, which is verified through Hall measurements. The hall measurement utilizes typical van der Waals method with four electrodes fabricated at four corners, as shown in Figure S4.

(a)

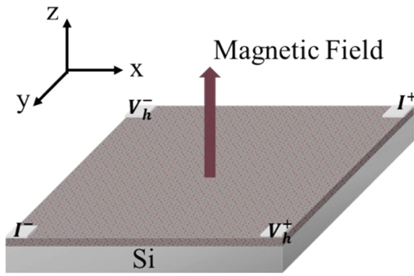

(b)

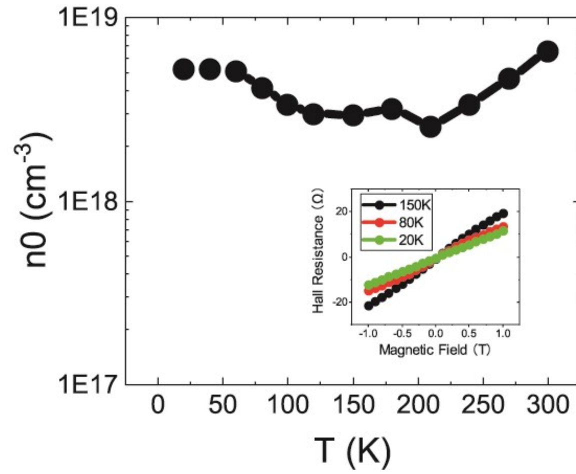

Figure S4: The Hall measurement. (a) Schematic diagram of Er/O/B doped sample with Hall electrodes. (b) Extracted electron concentration using Hall measurements at different temperatures (20K-300K). Inset shows the Hall resistance versus magnetic field curves at 150K, 80K, 20K, respectively.

VI Silicon band-edge emission vs Er emission

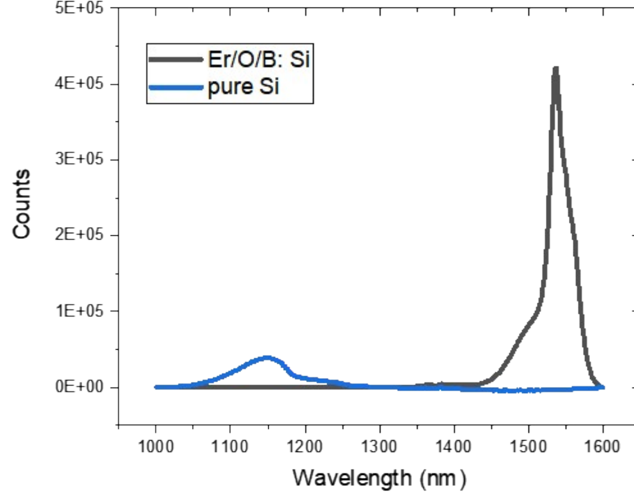

Figure S5: The emission spectrum of pure silicon wafer (blue curve) and Er/O/B: c-Si sample (black curve) under 405nm pumping photoflux density 5.5×10^{18} $s^{-1}cm^{-2}$ at 300K.

VII Derivations of energy transfer efficiency η_{ex}

When temperature T is low enough, term $W_{SRH}W_d$ approaches zero, then $\frac{1}{\phi_{out}}$ approaches $\frac{1}{\phi_0} = AW_0W_{fd}$. Furtherly,

$$\frac{W_0}{W_d}\left(\frac{1}{\phi_{out}} - \frac{1}{\phi_0}\right) = AW_0W_{SRH} \quad (18)$$

Then we have

$$\frac{W_{fd}}{W_{SRH}} = \frac{\frac{1}{\phi_0}}{\frac{W_0}{W_d}\left(\frac{1}{\phi_{out}} - \frac{1}{\phi_0}\right)} \quad (19)$$

Thus, energy transfer efficiency η_{ex} should be

$$\eta_{ex} = \frac{\frac{W_{fd}}{W_{SRH}}}{\frac{W_{fd}}{W_{SRH}} + 1} \quad (20)$$

VIII Calibration of system collection efficiency C

In order to obtain the absolute PLQY of our samples, the collection coefficient C of our PL system is calibrated using a commercial infrared LED (Hamamatsu, L12509-0155G, 1550nm) with a known emission power. The luminescence spectrum and far-field angular distribution are shown in Figure S5. Our sample has similar PL spectrum (measured experimentally) and far-filed emission profile (simulated by FDTD STACK solver) so that the calibrated collection coefficient C can be well applied in our sample to estimate its emission power.

The calibration process are as follows. As is shown in Figure S6, PL integrated intensities of the LED at different injection current were firstly measured in our PL system (the black dots). Then experimental data is scaled (red dots) by a factor of 2.31×10^{-3} to fit with a certificated power-current curve (red curve). Then the factor 2.31×10^{-3} is considered as the system conversion coefficient from arbitrary unit to Watt. Finally, the output photoflux density can be furtherly calculated with the known sample illumination area (or emission area) which is $1.6mm^2$.

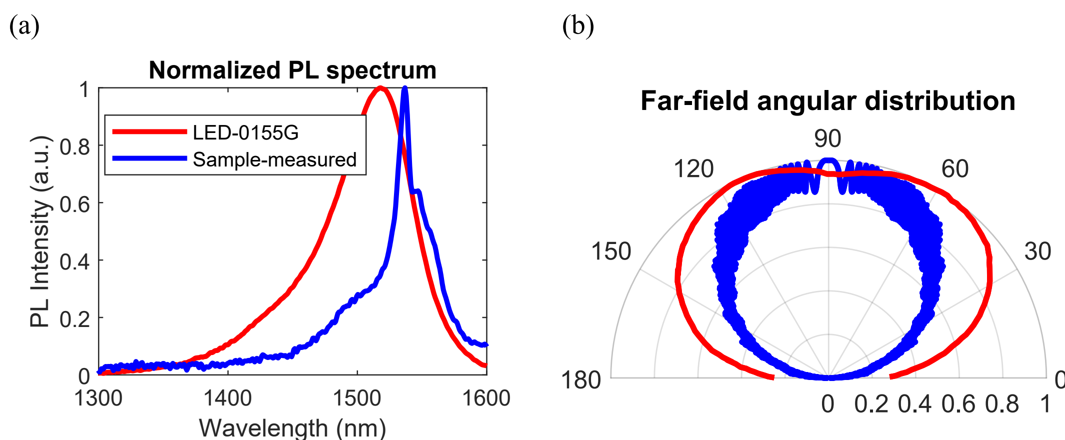

Figure S6: Comparison between commercial LED (Hamamatsu Cop L12509-0155G) and Er-doped Si. (a) Emission spectrums and (b) far-field angular distributions of the LED (red line) and crystalline Si (thickness 525μm, simulated using FDTD STACK) in the air (blue line).

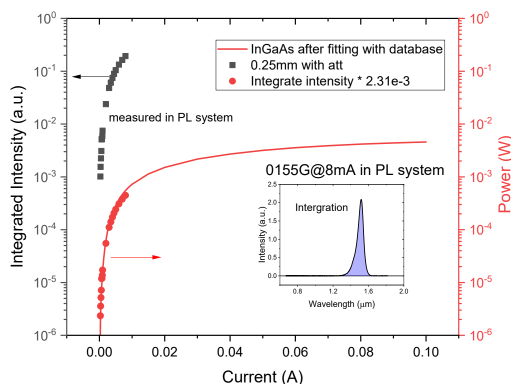

Figure S7: Calibration of system collection coefficient. The black dots indicate the measured PL integrated intensity in FTIR system (with arbitrary unit). The red curve is the absolute emission power-current curve provided in the LED datasheet. The red dots are the results of black dots scaled by a factor

of 2.31 ×10^{-3}. Inset shows the emission spectrum of the LED measured in our PL system.

The other factor that should be considered is the light extraction efficiency for our sample. For silicon (refractive index $n_{Si} = 3.4$), light extraction efficiency η_{out} can be estimated using Fresnel formula (for simplicity, we ignore internal multi-reflection).
Firstly, the critical angle for total internal reflection from silicon to air is

$$\varphi_c = \arcsin\frac{n_{air}}{n_{Si}} \approx 17°$$

Only light within this angle can emit and collected by detector. For this small φ_c, it corresponds to a solid angle Ω as

$$\Omega = \pi\varphi_c^2 = 0.088\pi\ (sr)$$

If we assume that Er can emit photons in arbitrary direction, which is reasonable due to the random distribution of Er centers. Then only $\frac{\Omega}{4\pi} = 2.2\%$ light can go through the Si/Air interface. Besides, this portion of light will be partly reflected. The final light extraction efficiency would be

$$EE = 2.2\% \times \frac{4n_{air}n_{Si}}{(n_{air} + n_{Si})^2} = 2.2\% \times \frac{4 \times 3.4}{4.4^2} = 1.5\%$$

, if the normal incidence is considered. This is only a rough estimation.
The result above can also be verified using Lumerical FDTD STACK solver. The simulated extraction efficiency within the range of 1450nm-1600nm is shown in Figure S7. Next, considering the PL spectrum of our samples (Figure S5. a) and the Er concentration depth profile below, the average light extraction efficiency can be calculated by integrations along the wavelength and depth dimensions,

$$\bar{EE} = \frac{\int_0^{200} Er(d) \int_{1450}^{1600} EE(\lambda,d)I(\lambda)d\lambda dEr}{\int_0^{200} Er(d) \int_{1450}^{1600} I(\lambda)d\lambda dEr} \approx 2.3\%$$

The average light extraction efficiency is about 2.3%, very close to the 1.5% we estimate. Therefore, it's acceptable to believe that only around 1/50 photons generated in our sample can emit out of the surface and then be collected with efficiency C. Thus, in order to obtain the PLQY, a factor of 50 should be multiplied.

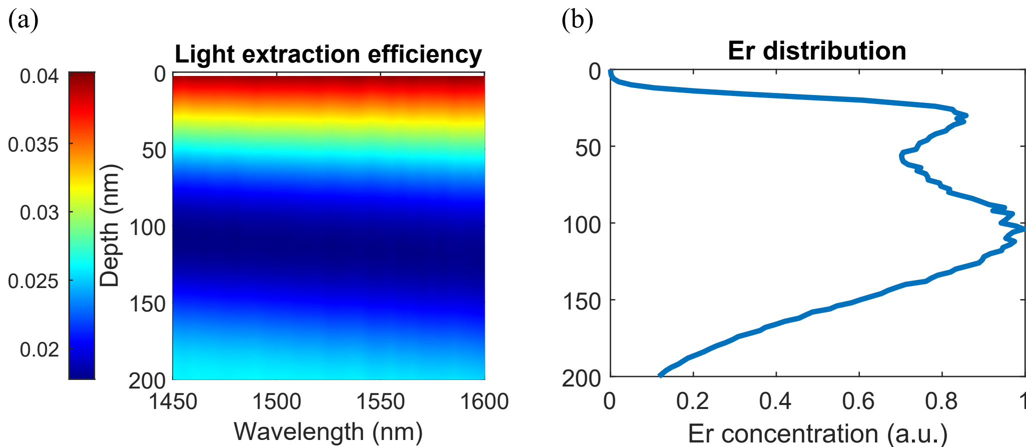

Figure S8: FDTD Stack simulation results. (a) Extraction efficiency of single Si layer (525μm) in the air for wavelength 1450-1600nm and Er centers located at different depths from the Si/Air interface. (b) The Er distribution at different depth from the surface.